GEOPHYSICAL RESEARCH LETTERS, VOL. 30, NO. 22, 2150, doi:10.1029/2003GL017743, 2003

Measuring ocean wave period with satellite altimeters: A simple empirical model

C. P. Gommenginger, M. A. Srokosz, and P. G. Challenor
Southampton Oceanography Centre, Europen Way, Southampton, UK

P. D. Cotton
Satellite Observing Systems, Godalming, UK

Received 14 May 2003; revised 20 August 2003; accepted 29 September 2003; published 21 November 2003.

[1] A simple empirical model is proposed to retrieve wave period from Ku-band radar altimeter backscatter and significant wave height. The model formulation is heuristic, and fitted using a large dataset of collocated Topex altimeter and buoys measurements. Empirical models are proposed for the zero up-crossing, the mean and the peak wave period, and compared with models by *Davies et al.* [1997] and *Hwang et al.* [1998]. Their performance is assessed using an independent validation dataset, and gives a retrieval error of 0.8s. Regional analysis indicates that the wave period models perform better in wind seas than in swell-dominated conditions. *INDEX TERMS:* 4275 Oceanography: General: Remote sensing and electromagnetic processes (0689); 4560 Oceanography: Physical: Surface waves and tides (1255); 4247 Oceanography: General: Marine meteorology. **Citation:** Gommenginger, C. P., M. A. Srokosz, P. G. Challenor, and P. D. Cotton, Measuring ocean wave period with satellite altimeters: A simple empirical model, *Geophys. Res. Lett.*, *30*(22), 2150, doi:10.1029/2003GL017743, 2003.

1. Introduction

[2] Satellite altimeters provide global data on ocean mean sea level (MSL), significant wave height (SWH) and wind speed (U_{10}). Altimeter U_{10}, derived from the radar backscatter coefficient σ^0, has long been known for its sensitivity to sea state development [*Glazman and Pilorz*, 1990]. A number of altimeter wind speed models have been proposed [e.g., *Gourrion et al.*, 2002] to account for sea state development biases, but a residual bias dependent on sea state development is known to persist even for retrieval models based on SWH and σ^0 [*Gommenginger et al.*, 2002].

[3] The sensitivity of nadir altimeters to sea state offers however an opportunity to retrieve much-wanted information on wave conditions, in addition to SWH. Altimeter SWH is presently the only sea state parameter available globally from space-borne instruments, and is used extensively in numerical ocean wave prediction models, even though SWH is a poor sea state descriptor on its own. The availability of global spectral information would enhance the reliability of numerical wave model forecasts. In principle, directional wave spectra can be obtained from synthetic aperture radars (SAR), but unresolved issues about SAR imaging of ocean waves mean routine extraction of wave spectra from SAR has not been pursued to-date. Hence, global wave period data is not presently available, except from numerical wave models.

[4] The retrieval of wave period from altimeters has so far received little attention. Two previous studies, *Davies et al.* [1997; hereafter D97] and *Hwang et al.* [1998; hereafter H98], proposed altimeter wave period models, but in both, the sea state dependence of the model is complex and the models were received with scepticism. The D97 model uses theoretical arguments for its formulation, but then includes a strongly non-linear dependence on altimeter-derived pseudo-wave age [*Fu and Glazman*, 1991] with coefficients obtained by fitting a small dataset of collocated ERS-1/buoy data. In turn, H98 assumes a number of relationships between peak frequency, fetch and total wave energy, which restrict the range of applicability of the model. In both cases, retrieval accuracies around 0.5s (r.m.s.) were reported, although environmental conditions in the validation datasets were limited, either geographically (H98, to the Gulf of Mexico), or in time (D97, by using only two years of altimeter data). Here, we try to avoid such pitfalls by adopting a simple empirical approach, based on heuristic reasoning and a large dataset of ocean wave spectra collocated with Topex altimeter data.

2. Collocated Buoy/Topex Dataset

[5] The buoy data originates from the US National Data Buoy Center (NDBC) who provide one-directional buoy spectra for a large number of moored buoys around the U.S. coast. The buoys used here were selected for their location in open water and proximity to Topex tracks. A network of 24 buoys provides a reasonable representation of the global wave field [*Gommenginger et al.*, 2002], although information is lacking in the southern hemisphere.

[6] In contrast to our previous wind studies [*Gommenginger et al.*, 2002] where buoy/Topex space separation was set to 50 km, we used a less stringent separation of 100 km to account for the larger scales of variability of the wave field. The maximum time separation between Topex and buoy data is 1 hour. With these criteria and the application of standard ice and rain flags from the AVISO Topex geophysical data records (GDR), the collocation yielded 6344 data points for the period September 1992–December 1998. The data consist of Topex Ku-band backscatter coefficient and SWH, chosen as the 1 Hz altimeter record located closest to the buoy within a 100 km radius. No attempt was made to compensate for the gradual drift in Topex's estimates towards the end of

0094-8276/03/2003GL017743$05.00

1998, as this drift was previously shown to have no perceptible impact in our dataset [*Gommenginger et al.*, 2002]. The buoy data include wind speed and direction, SWH, air and sea temperatures, and peak (T_p) wave period from the NDBC metocean parameter records, and one-dimensional frequency wave spectra from the NDBC spectral records. Mean (T_m) and zero-crossing period (T_z) were computed from the moments of the one-dimensional ocean wave spectra with [*Tucker*, 1991]:

$$T_m = m_0/m_1 \qquad \text{and} \qquad T_z = (m_0/m_2)^{1/2} \tag{1}$$

3. Empirical Altimeter Wave Period Model

[7] Our empirical model is based on heuristic reasoning and, unlike previous altimeter wave period models, makes no assumptions on, for example, the shape of the ocean wave spectrum. At nadir, σ^0 is related under the Geometrical Optics approximation to the inverse of the mean square slope (mss) of the long ocean waves [*Barrick*, 1974]:

$$\sigma^0 \sim mss^{-1} \tag{2}$$

In turn, wave slope is dimensionally equivalent to the ratio of some measure of the wave height and the wavelength, L:

$$slope \sim SWH/L \tag{3}$$

The ocean wavelength is related to wave period, T, through the dispersion relationship for deep water gravity waves, so that $L \sim T^2$ and $mss \sim SWH^2/T^4$, and thus:

$$T \sim \left(\sigma^0 SWH^2\right)^{0.25} \tag{4}$$

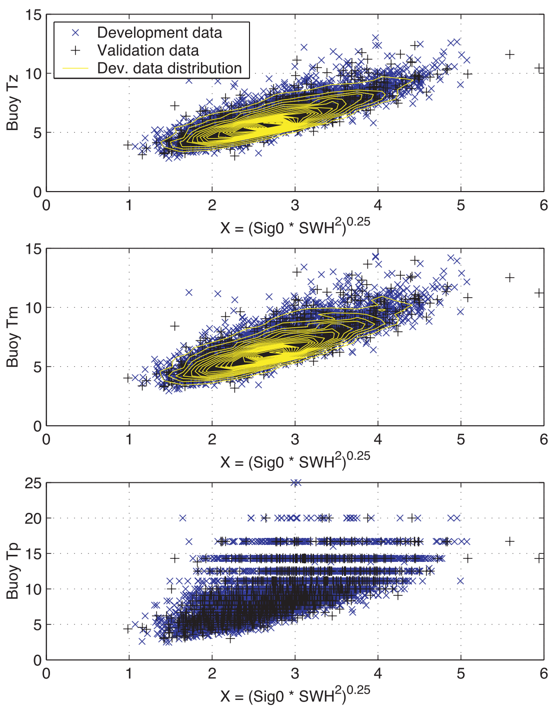

Figure 1. Buoy T_z, T_m and T_p versus X for collocated dataset. Contour lines show the density of data points. See color version of this figure in the HTML.

Table 1. ODR Coefficients for Empirical Wave Period Models Applied to the Development Dataset (5075 Data Points)

	a (±95%)	b (±95%)
$T_z = a + b\,X$	− 0.895 (± 0.126)	2.545 (± 0.045)
$\log_{10}(T_z) = a + b * \log_{10}(X)$	0.361 (± 0.007)	0.967 (± 0.016)
$\log_{10}(T_m) = a + b * \log_{10}(X)$	0.352 (± 0.008)	1.063 (± 0.019)
$\log_{10}(T_p) = a + b * \log_{10}(X)$	0.154 (± 0.021)	1.797 (±0.047)

[8] Simple empirical models were constructed for T_z, T_m, and T_p, all based on equation (4). Figure 1 shows the buoy T_z, T_m and T_p against $X = (\sigma^0 * SWH^2)^{0.25}$ calculated from the Topex data. The contour lines indicate the density of data points, and show a strong correlation with X for both T_z and T_m. Simple empirical models were built by performing linear regressions of wave period against X. For this, the collocated dataset was divided into a development dataset (5075 points) for the determination of the fitted coefficients, and a validation dataset (1269 points), extracted at random from the original dataset.

[9] Figure 1 also illustrates the problems of using T_p as a sea state descriptor. It is clear that T_p is an unstable parameter, especially at large periods. One can discern in the buoy T_p data the log-spaced discrete frequency bands used to report the buoy one-directional wave spectra from which T_p is derived. This contrasts sharply with T_z and T_m, which, as integrals of the spectrum, are more stable and thus preferable parameters to characterise sea state. For the sake of completeness, we nonetheless develop an empirical model for T_p, although the quantisation of T_p will impact both the quality of the model and any assessment based on the validation data.

[10] The linear regression of wave period against X was performed using Orthogonal Distance Regression (ODR; [*Boggs and Rogers*, 1990]), with X calculated with the altimeter σ^0 expressed in its linear (non-dB) form. Using ODR enables us to consider errors in both T and X, but forces us to assume that the variances of the errors in T and X are equal. This is difficult to justify and means that our results are not invariant with scaling. However, we believe our results to be robust, and defer the use of a better statistical technique to a future paper. Further improvement from the simple linear fit was achieved by fitting the wave period against X in log-log space. There are two advantages to this approach: firstly, the distribution of log(SWH) is closer to a normal distribution than that of SWH; secondly, any constant offset in dB in the (un-calibrated) σ^0 gets absorbed in the estimate of the fitted offset "a" in the linear regression. The fitted coefficients, and their 95% confidence intervals, are given in Table 1.

4. Assessment of Altimeter Wave Period Models

[11] We start by examining the behaviour against U_{10} and SWH of the empirical log-log, D97 and H98 models for T_z (Figure 2). Comparison with D97 requires the adjustment of Topex σ^0 to ERS-1 levels. Since ERS-1 σ^0 were aligned with Geosat, Topex σ^0 values were adjusted to Geosat/ERS-1 levels using the −0.63 dB correction suggested by *Callahan et al.* [1994].

[12] The empirical log-log and H98 models for T_z display physically sound behaviour, with similar monotonic trends with SWH and U_{10}. Both models also mimic the quadratic

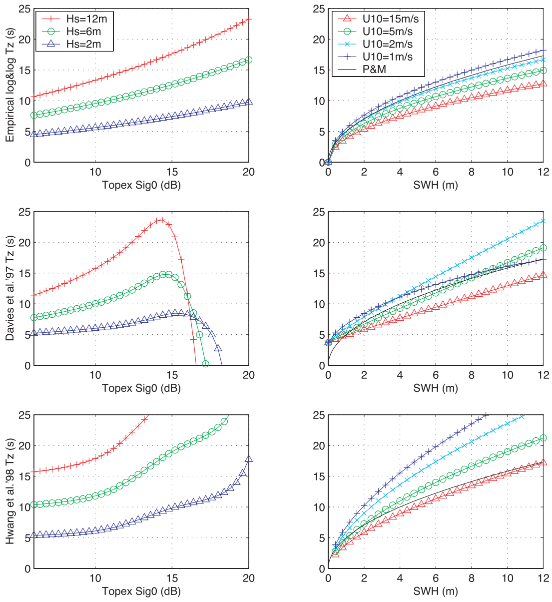

Figure 2. Physical trends of the empirical log-log, *Davies et al.* [1997], and *Hwang et al.* [1998] models for T_z against U_{10} (or $\sigma 0$) and SWH. See color version of this figure in the HTML.

relation between wave period and SWH obtained for the Pierson-Moskowitz spectrum for fully developed seas [*Carter*, 1982]. In contrast, D97 shows a marked non-physical behaviour for σ^0 values larger than about 14 dB (i.e., low wind speeds). This feature results from the model's strongly non-linear formulation and the limited collocated ERS-1/buoy dataset used to develop the model, where few low wind conditions were available [*Davies et al.*, 1997]. Hereafter, we avoid this problem by implementing D97 only for Topex σ^0 below 14 dB. A second limiting feature of D97 is seen in its dependence on SWH, where for small SWH, the model cannot return wave periods less than 4s. This has also been linked to the restricted range of conditions in the ERS-1/buoy dataset.

[13] Next, the performance of all models is evaluated using the statistics of the residual wave period error defined as $dT = T_{Buoy} - T_{Alt}$, where T refers to T_z, T_m or T_p (Table 2). For the independent validation dataset, the (linear) empirical and the D97 models for T_z return an r.m.s. error around 0.9s, while the empirical log-log model for T_z returns an error under 0.8s. While the empirical models for T_z display no bias, D97 shows a large, unexplained, -0.52s bias. H98 performs yet worse both in terms of bias and r.m.s. error. The empirical log-log model for T_m shows a retrieval error of about 1s. Models for T_p return errors in excess of 2.8s and large biases, explained partly by the noisy nature of the T_p buoy data.

[14] To understand the performance of the different models in various sea conditions, we identified, within the validation dataset, data for the Gulf of Mexico (266 points) and the Hawaii (268 points) regions, and repeated the above analysis. The Gulf of Mexico subset typifies enclosed sea conditions, generally dominated by wind waves, while the Hawaii subset typically includes swell. In Table 2, the empirical models for T_z and T_m perform better when tested on the Gulf of Mexico data alone, and worse for the Hawaii dataset alone. This suggests that the empirical models are better suited to wind-sea than to swell conditions. For the Gulf of Mexico, the r.m.s. error for the empirical models is about 0.6s for T_z and 0.7s for T_m. Similar trends are seen for H98, in line with the H98 model having been developed specifically for the Gulf of Mexico region. The picture is less clear for D97, for which the standard deviation improves only slightly for the Gulf of Mexico, while its bias degrades to -0.8 s. It is conceivable that D97 might have performed better if its empirical coefficients had been re-fitted using the present dataset, but this will not be explored here. In all cases, the improved performance of the T_p models in the Gulf of Mexico is due primarily to the smaller wave period conditions prevalent in this region, for which the discrete buoy frequency band problem identified in Figure 1 is less important.

[15] We now consider residual trends in T_z against various parameters, including X, buoy wave period and buoy U_{10} (Figure 3). This reveals a number of residual dependences, in particular with U_{10}. Of concern is the residual dependence on the fitted parameter X for the log-log empirical model, which is not present in the D97 model. Thus, the empirical log-log model underestimates T_z for small values of X (i.e., high winds and/or small SWH) and overestimates T_z for large values of X (i.e., low winds and/or large SWH). The residuals for D97 confirm an overall negative bias. There is evidence also of truncation, which is related to D97's inability to return values of T_z smaller than 4s. The residuals against U_{10} for both models, but particularly for the empirical T_z model, display an interesting change in behaviour around U_{10} = 3 m/s. This may be resolved for the empirical T_z model by using a more complex fitted model. Alternatively, it may be evidence of a real physical effect in different wind speed regimes.

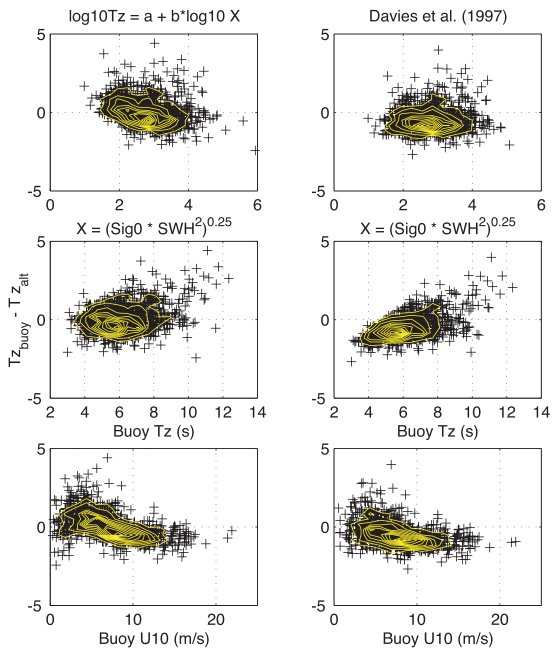

Figure 3. Residual error $T_{zBuoy} - T_{zAlt}$ for the empirical log-log and *Davies et al* [1997] model, against X, buoy T_z, and buoy U_{10}. Contour lines show the density of data points. See color version of this figure in the HTML.

Table 2. Residual Statistics for (Top) the Development and the Validation Datasets (Bottom) Validation Data in the Gulf of Mexico and Hawaii Regions

		Development dataset				Validation dataset			
		N	Bias	rmse	Sdev	N	Bias	rmse	Sdev
T_z	$T_z = a + b X$	5075	−0.000	0.871	0.871	1269	−0.009	0.900	0.900
	$\log_{10}T_z = a + b * \log_{10}X$	5075	0.005	0.785	0.785	1269	−0.008	0.797	0.797
T_m	$\log_{10}T_m = a + b* \log_{10}X$	5075	0.000	0.965	0.965	1269	−0.010	0.988	0.988
T_p	$\log_{10}T_p = a + b * \log_{10}X$	5075	−0.216	3.046	3.038	1269	−0.223	3.060	3.052
Davies et al. [1997]	T_z	4742	−0.519	0.856	0.680	1194	−0.525	0.876	0.701
Hwang et al. [1998]	T_z	5075	−0.922	1.362	1.002	1269	−0.926	1.442	1.105
	T_p	5075	0.518	2.674	2.623	1269	0.497	2.859	2.816
		Gulf of Mexico (Validation)				Hawaii (Validation)			
		N	Bias	rmse	Sdev	N	Bias	rmse	Sdev
T_z	$\log_{10}T_z = a + b * \log_{10}X$	266	−0.014	0.608	0.608	268	−0.121	0.853	0.844
T_m	$\log_{10}T_m = a + b* \log_{10}X$	266	−0.058	0.709	0.707	268	−0.009	1.093	1.092
T_p	$\log_{10}T_p = a + b * \log_{10}X$	266	0.345	1.730	1.695	268	0.038	3.177	3.177
Davies et al. [1997]	T_z	249	−0.804	0.937	0.482	260	−0.464	0.904	0.776
Hwang et al. [1998]	T_z	266	−0.466	0.955	0.833	268	−1.198	1.649	1.134
	T_p	266	−0.099	1.763	1.760	268	1.215	3.838	3.640

Note that the bias, root-mean-square error (rmse) and standard deviation (Sdev) are all expressed in seconds. N represents the number of valid points for each model.

[16] Finally, Figure 4 shows the histograms of the altimeter retrieved T_z and T_m for the various models with respect to the buoy data. To obtain meaningful distributions, the analysis used the whole collocated dataset, and thus does not represent a fully independent test of the empirical models. In the absence of additional wave period data, it nevertheless provides useful information about the global retrieval abilities of each model. The top subplot shows D97's difficulty in returning wave periods below 4s. We note that this feature is not related to the 14 dB cut-off in σ^0 applied to eliminate non-physical behaviour of the D97 model. In the absence of such data flagging, the D97 wave period histogram features another 400 strongly negative or near-zero values, but still displays the abrupt cut-off at 4s. The wave period histogram for H98 (T_z) also compares poorly with the buoy measurements. In contrast, the histogram for the empirical log-log T_z model shows good agreement with the buoy T_z histogram, except near the peak. Thus, the empirical model fails to capture fully the behaviour of the buoy data where the density of measurements is maximal. The bottom subplot in Figure 4 represents the same analysis for T_m, and shows similar results.

5. Conclusions

[17] A new, simple empirical algorithm was proposed to relate, to a first approximation, the ocean wave period to nadir altimeters' Ku-band σ^0 and SWH measurements. The formulation of the model was derived heuristically, and uncovered a strong link between wave period and the quantity X defined as $(\sigma^0 * SWH^2)^{0.25}$. Using a large dataset of Topex measurements collocated with one-dimensional buoy wave spectra, simple wave period models were developed and tested for T_z, T_m and T_p, and compared with existing models by *Davies et al.* [1997] and *Hwang et al.* [1998].

[18] Validation, based on a subset of independent measurements, indicates that wave period can be retrieved globally from altimeter data with an r.m.s. error of the order of 0.8s for T_z. Analysis of the altimeter models' performance in different sea conditions suggest that they are better suited to wind-dominated seas than to regions with swell. Some residual dependence was found against various geophysical parameters, which may be addressed for the empirical approach with a more complex fitted model.

[19] Overall, we found that, unlike previous wave period models, the simple empirical models are better able to reproduce the wide range of wave period conditions seen in our collocated Topex/buoy dataset. Lessons should be learned from D97 though, where the restricted range of wind/wave conditions in the collocated altimeter/buoy dataset led to severe limitations of the model. Therefore, much validation remains to be done, especially with regards to testing the empirical models with data from the Southern Ocean and the coastal zone.

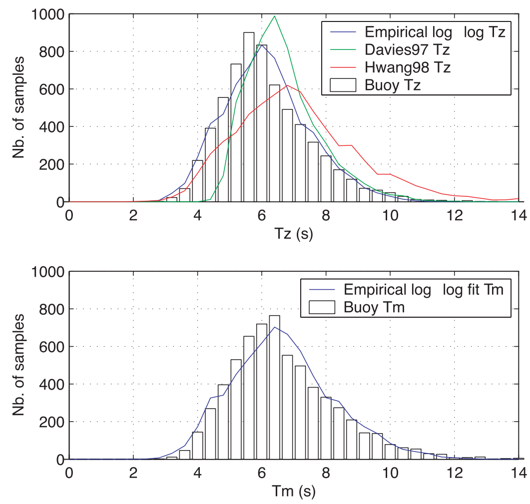

Figure 4. Histograms of retrieved wave period for (top) T_z from empirical log-log, *Davies et al.* [1997], and *Hwang et al.* [1998] models, and (bottom) T_m for empirical log-log model, against buoy wave period histogram. See color version of this figure in the HTML.

References

Barrick, D. E., Wind dependence of quasi-specular microwave sea scatter, *IEEE Trans. Antenna Prop.*, AP-22, 135–136, 1974.

Boggs, P. T., and J. E. Rogers, Orthogonal distance regression, in *Contemporary Mathematics*, Volume 112, edited by P. J. Brown and W. A. Fuller, pp. 183–194, *Am. Math. Soc.*, 1990.

Callahan, P. S., C. S. Morris, and S. V. Hsiao, Comparison of Topex-Poseidon σ0 and significant wave height distributions to Geosat, *J. Geophys. Res.*, *99*, 25,015–25,024, 1994.

Carter, D. J. T., Predictions of wave height and period for a constant wind velocity using the Jonswap results, *Ocean Eng.*, *9*, 17–33, 1982.

Davies, C. G., P. G. Challenor, and P. D. Cotton, Measurement of wave period from radar altimeters, in *Ocean wave measurement and analysis*, edited by B. L. Edge and J. M. Hemsley, pp. 819–826, *Am. Soc. Civil Eng.*, USA, 1997.

Fu, L.-L., and R. E. Glazman, The effect of the degree of development on the sea state bias in radar altimetry measurement, *J. Geophys. Res.*, *96*(C1), 829–834, 1991.

Glazman, R. E., and S. H. Pilorz, Effects of sea maturity on satellite altimeter measurements, *J. Geophys. Res.*, *95*, 2857–2870, 1990.

Gommenginger, C. P., M. A. Srokosz, P. G. Challenor, and P. D. Cotton, Development and validation of altimeter wind speed algorithms using an extended collocated buoy/Topex dataset, *IEEE Trans. Geosc. Remote Sens.*, *40*(2), 251–260, 2002.

Gourrion, J., D. Vandemark, S. A. Bailey, B. Chapron, C. P. Gommenginger, P. G. Challenor, and M. A. Srokosz, A two parameter wind speed algorithm for Ku-band altimeters, *J. Atmos. Ocean Tech.*, *19*(12), 2030–2048, 2002.

Hwang, P. A., W. J. Teague, G. A. Jacobs, and D. W. Wang, A statistical comparison of wind speed, wave height and wave period derived from satellite altimeters and ocean buoys in the Gulf of Mexico region, *J. Geophys. Res.*, *103*, 10,451–10,468, 1998.

Tucker, M. J., Waves in ocean engineering: Measurement, analysis, interpretation, 431 pp., Ellis Horwood Ltd., Chichester, England, 1991.

C. P. Gommenginger, M. A. Srokosz, and P. G. Challenor, Southampton Oceanography Centre, European Way, Southampton, UK. (cg1@soc.soton.ac.uk)

P. D. Cotton, Satellite Observing Systems, Godalming, UK.